Bull. Inst. Chem. Res., Kyoto Univ., Vol. 59, No. 4, 1981

Microheterophase Structure, Permeability, and Biocompatibility of A-B-A Tri-Block Copolymer Membranes Composed of Poly (γ-ethyl *L*-glutamate) as the A Component and Polybutadiene as the B Component

Guan-Wen CHEN*, Hiroko SATO**, Toshio HAYASHI**, Kohei KUGO***, Yasuharu NOISHIKI****, and Akio NAKAJIMA***

Received July 14, 1981

A–B–A block copolymers consisting of poly(γ-ethyl L-glutamate) as the A component and Polybutadiene as the B component, designated as EBE, were synthesized. The microheterophase structure of these block copolymers observed by electron microscope was not so clear as that of block copolymers containing poly(γ-benzyl L-glutamate) as the A component, which was attributed to the better compatibility of ethyl group with polybutadiene. The water permeation through EBE block copolymer membranes was discussed. The EBE block copolymers were found out to have good biocompatibility.

KEY WORDS: Tri-block copolymer/ Microheterophase structure/ Membrane permeability/ Biocompatibility/

INTRODUCTION

In our previous papers,[1~3] the microheterophase structure and properties of A–B–A block copolymers (GBG) consisting of poly (γ-benzyl L-glutamate) as the A component and polybutadiene as the B component in chloroform, a helicogenic solvent, were discussed as a function of the polybutadiene content. The GBG membranes were found to have high water permeability despite of their low degree of swelling in water. It is very interesting to elucidate the mechanism of water permeation in block copolymer membranes containing polypeptides, depending on the kind of ester group included in polypeptide molecules.

In the preceding paper,[4] the A–B–A block copolymers, EBE, consisting of poly (γ-ethyl L-glutamate) as the A component and polybutadiene as the B component were synthesized in a similar manner as GBG block copolymer series, and their molecular characterization was performed.

In this paper, we will discuss the water permeability and the biocompatibility of EBE membranes in comparison with block copolymers MBM[5] containing poly(γ-methyl L-glutamate) as the A component. The ethyl ester of poly(L-glutamic acid) is expected not

* 陳 観 文：On leave from Institute of Chemistry, Chinese Academy of Sciences, Peking, China.
** 佐藤弘子，林 寿郎：Research Center for Medical Polymer and Biomaterials, Kyoto University, Kyoto.
*** 久後行平，中島章夫：Department of Polymer Chemistry, Faculty of Engineering, Kyoto University, Kyoto.
**** 野一色泰晴：Institute for Thermal Spring Research, Okayama University, Misasa, Tottori.

to be harmful *in vivo* even on the process of biodegradation and, hence, the EBE block copolymers will be designed particularly for biomedical uses.

EXPERIMENTAL

Materials

A homopolypeptide, poly(γ-ethyl L-glutamate) (designated as PELG), and A–B–A type block copolymers EBE composed of poly(γ-ethyl L-glutamate) as the A component and polybutadiene as the B component were synthesized[4] according to the method reported in the previous paper.[1] The *N*-carboxy anhydride of γ-ethyl L-glutamate (γ-ELG) was prepared from L-glutamic acid as a starting material. A cycloaliphatic secondary amine terminated polybutadiene (ATPB), the molecular weight of which was 3600, was used as the middle block for all the EBE block copolymers reported here.

The EBE block copolymers were prepared by the polymerization of various amounts of NCA of γ-ELG onto ATPB in a mixture of dioxane and methylene dichloride (1 : 2 v/v) at 20°C for 72 h. The molar percentage of γ-ELG in block copolymers was estimated from the results of elemental analysis in the Organic Microanalyses Center in Kyoto University and of the IR spectra.

IR, X-Ray Diffraction, and Electron Microscope Measurements

The IR spectra of block copolymer films were measured with a Shimadzu Model-30A infrared spectrophotometer. The compositions of block copolymers were calculated from the relative intensity at 970 cm^{-1} to that at 1120 cm^{-1}. Wide-angle X-ray diffraction of polymer films was measured with a Rigaku Geigerflex type DF-3 X-ray generator, equipped with an automatic diffractometer, where Ni-filtered Cu-Kα radiation was set so as to radiate onto a flat surface of the film parallel to the reflecting surface. Thin films of block copolymers formed on cupper mesh were stained with osmic tetraoxide. The domain structures of A–B–A tri-block copolymers were observed by a Hitachi High Resolution Transmission Electron Microscope H-500.

Permeability Measurement

For the purpose of membrane preparation, about 2% polymer solution, whose solvent was a mixture of chloroform and trifluoroethanol, was cast onto glass plate, and dried at room temperature. The membrane thickness obtained was 20 to 30 μm. The degree of swelling of membrane was measured with a microbalance manufactured by Chyo Balance Co. (Kyoto).

The hydraulic permeability of the membranes, set on porous supporter, was measured with a low-pressure ultrafiltration apparatus Model MC-II made by Bio-Engineering Co. at various temperatures from 25 to 50°C under various pressures from 1 to 4 atm. The flux of effluent was evaluated during some period by weighing the volume of the effluent through membrane of 12.57 cm^2.

Test of Biocompatibility

Polymer samples coated on the mesh cloth of polyester fiber were implanted subcutaneously in rabbits for 4 weeks, and then tissue compatibility was observed by the same method[6] as that for polypeptide block copolymer membranes containing poly(γ-benzyl L-glutamate), poly(γ-methyl L-glutamate), or poly(ε-*N*-carbobenzyloxy L-lysine).

The polyester mesh of 1×3 cm in size was dipped in ethyl alcohol for 24 h in order to remove lubricant and plasticizer in the polyester fiber, washed in pure water, and dried. Such polyester mesh served as a supporter of thin polymer film of *ca.* 20 μm in thickness, and a marker of polymer samples implanted in the tissue, as well as a reference of polymers for biocompatibility reaction. The 1.6% polymer solutions of EBE in a mixture of chloroform and trifluoroethanol (4 : 1 v/v) were cast on the polyester mesh and air-dried.

After washed in pure water, polymer samples coated on the polyester mesh were sterilized by immersing in 70% ethyl alcohol aqueous solution for one week, and then dipped in a physiological salt solution before the implantation. The samples, implanted in the muscle tissue on the back of rabbits for 4 weeks, were taken out together with the tissue around the polymer samples. The specimens obtained after fixation in 10% formalin were incubated in paraffin. The sliced specimens, stained with hematoxylin and eosin, were examined microscopically.

RESULTS AND DISCUSSION

Wide Angle X-Ray Diffraction

The orientation of α-helical polypeptide molecules in unstretched PELG and EBE films, cast from mixing solvent of chloroform and trifluoroethanol (2 : 1 v/v), was investigated with X-ray diffraction patterns on the (1 $\bar{1}$ 0) plane. The composition of polypeptides, A mole%, in those polymer is listed in Table I, together with P_A and X_H, in which P_A and X_H mean the degree of polymerization of the A component and the helical content,[4] respectively.

Figure 1 shows the wide-angle X-ray diffraction (WAXD) patterns for PELG and EBE block copolymer films. The diffraction peaks at 2θ of ca 7.5° become broader with increasing the polybutadiene content in block copolymers, which means the less crystallinity and worse orientation of α-helix in EBE films with increasing polybutadiene content.

The main diffraction peak of PELG at 2θ of 7.25° corresponds to an intermolecular

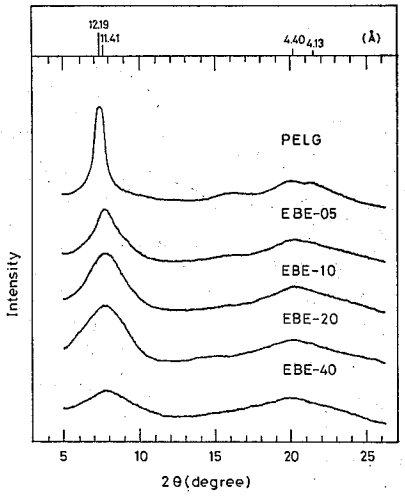

Fig. 1. Wide-angle X-ray diffraction profiles of unoriented PELG and EBE solid films.

Table I. Molecular parameters of PELG and EBE

Code	A (mole%)	P_A	X_H
PELG–2	100	588	1
EBE–05	94.5	495	0.95
EBE–10	89.5	260	0.89
EBE–20	80.6	127	0.80
EBE–40	60.5	47	0.60
EBE–70	31.5	14	

spacing 12.19 Å of the PELG chains in homopolypeptide film, while the 2θ of the main diffraction peak and the intermolecular spacing for EBE films are 7.75° and 11.41 Å, respectively. The phenomenon that the existence of polybutadiene in block copolymers results in shorter intermolecular spacing of α-helix than that in homopolypeptide film was observed with MBM[5] and EBE copolymers, but not with GBG copolymers.[1] The intermolecular spacing of α-helices in polypeptide films is influenced by casting solvent in the film preparation,[1,7] because solvent affects the packing of side chains in polypeptide molecules. The smaller intermolecular spacing by 0.78 Å in EBE films composed with that in PELG homopolymer film may be due to better compatibility of polybutadiene with aliphatic part of side chains such as ethyl and methyl residues.

From the analysis of X-ray diffraction paterns of PMLG, the unit cell of PMLG was concluded to be hexagonal according to Bamford and Hanby.[8] Assuming that the unit cell of PELG, having one longer methylene side chains than PMLG, is hexagonal like the PMLG unit cell, the cross sections of the unit cell of both PMLG and PELG are depicted in Fig. 2. The inner and the outer circles represent the core of α-helices and the whole helical chains, respectively, projected on the plane perpendicular to the fiber axis. On the basis of hexagonal unit cell of PELG, the packing helical diameter was calculated to be 14.08 Å. Valle *et al.*,[9] however, found from X-ray analysis of PELG cast from dichloroethan and dimethyl formamide that the unit cell of the PELG was pseudo-hexagonal,

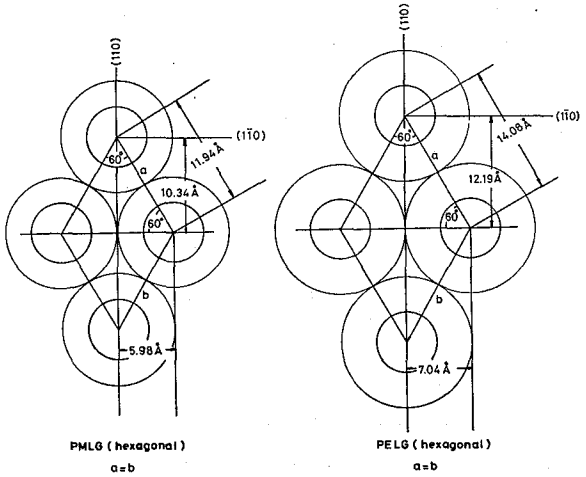

Fig. 2. Cross section of unit cells of PMLG and PELG.

monoclinic, and the packing helical diameter was calculated to be 12.5 Å. It was supposed that the inter-helical interactions by the long side chains caused the deviation of PELG from the hexagonal to be monoclinic packing.

Formation of Microheterophase Structure

As is obvious from Table I, A-block chain portion of EBE copolymers takes α-helix conformation in helicogenic solvent. Further, polybutadiene exists in random coil conformation in solution. Thus, the molecular conformation of EBE copolymers in solution is represented by Fig. 3, where a is the radius of cross section of an α-helix, and h is the residue translation in the α-helix. A B-chain is divided into two unit chains connected at the midpoint M of the B-chain, and the root mean square end-to-end distance and the root mean square radius of gyration of the unit chain having a degree of polymerization of $P_B/2$ are denoted by $\langle r_{B/2}^2\rangle^{1/2}$ and $\langle s_{B/2}^2\rangle^{1/2}$, respectively. Thus an A–B–A tri-block chain is assumed to be composed of two A-(B/2) di-block chains connected at the point M.

At the critical micelle concentration, the A–B–A block copolymer undergoes microphase separation and aggregates into micelles, such as spherical, cylindrical, and lamella-like micelles, as illustrated in Fig. 4, in accordance with the copolymer composition, dimension of blocks, and environmental conditions.

The Gibbs free energy ΔG per unit volume for the micelle formation is given by

$$\Delta G=\Gamma\Delta W-T\Delta S \tag{1}$$

where Γ is the area of A/B interface per unit volume of micelle, ΔW (erg/cm²) is the interfacial free energy per unit area of A/B interface and is equal to the interfacial tension γ_{AB} (dyne/cm), and ΔS is the entropy change accompanied by the micelle formation. According to Nakajima *et al.*,[2] the equilibrium micelle dimensions, $D_{s,eq}$, $D_{c,eq}$, and L_{eq}, respectively, for spherical, cylindrical, and lamella-like micelles, are given by the following equations.

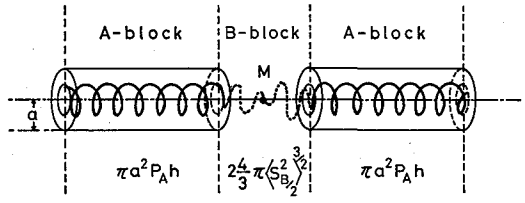

Fig. 3. Molecular conformation of EBE in helicogenic solvent.

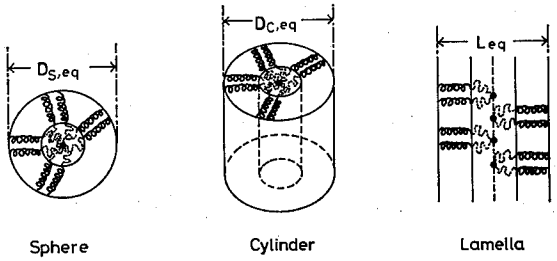

Fig. 4. Micelles formed from A–B–A block polymer solutions at critical concentration.

Table II. Micelle dimensions of EBE block polymers

Code	ϕ_B	$D_{s,eq}$(Å)	$D_{c,eq}$(Å)	L_{eq}(Å)	D_{EM}(Å)
EBE-05	0.17	470			480 (sphere)
EBE-10	0.28		429		420 (cylinder)
EBE-20	0.44		341		380 (cylinder)
EBE-40	0.68			264	350 (lamella)
EBE-70	0.88			204	360 (lamella)

$$D_{s,eq}=\left[\frac{8\Delta W\langle r_{B/2}{}^2\rangle}{\mathrm{KT}N}\right]^{1/3} \tag{2}$$

$$D_{c,eq}=\left[\frac{16\Delta W\langle r_{B/2}{}^2\rangle}{3\phi_B{}^{1/2}\mathrm{kT}N}\right]^{1/3} \tag{3}$$

$$L_{eq}=\left[\frac{8\Delta W\langle r_{B/2}{}^2\rangle}{3\Phi_B{}^2\mathrm{kT}N}\right]^{1/3} \tag{4}$$

in which ϕ_B is the volume fraction of the domain occupied by B block to the total volume occupied by the copolymer, both in solution, given by Eq. (5).

$$\phi_B=\frac{(4/3)\pi\langle s_{B/2}{}^2\rangle^{3/2}}{(4/3)\pi\langle s_{B/2}{}^2\rangle^{3/2}+\pi a^2P_Ah} \tag{5}$$

and N is the number of junction points between A and B block per unit volume of micelle, *i.e.*, twice the number of block copolymer per unit volume of micelle, and given by

$$N=1/[(4/3)\pi\langle s_{B/2}{}^2\rangle^{3/2}+\pi a^2P_Ah] \tag{6}$$

Accordingly, if the numerical values of $\langle r_{B/2}{}^2\rangle$, $\langle s_{B/2}{}^2\rangle$, a, and ΔW are known, we can estimate the dimension of micelles from Eqs. (2), (3), and (4).

The solvent used for casting of membrane was a 4 : 1 mixture of chloroform (CF) and trifluoroethanol (TFE) in which the latter is more volatile than the former. Furthermore, the polybutadiene used was rich in *trans*-1,4-configuration. At critical micelle concentration, content of TFE in the solvent mixture may be regarded very low. So, the $\langle r_{B/2}{}^2\rangle$ and $\langle s_{B/2}{}^2\rangle$ were estimated from literature data[10,11] on poly(*trans*-1,4 butadiene)-chloroform system, as 41.34 Å, and 16.88 Å, respectively. The radius, a, of cross section of PELG helix was estimated as 6.58 Å, by using the intermolecular spacing 11.41 Å obtained from X-ray data.

With respect to interfacial tension γ_{AB} of PELG/poly(*trans*-1,4 butadiene) system, nothing has been reported. Hence, we used the value of 25.7×10^{-16} erg/Å for ΔW, which was obtained for PMLG/poly(*trans*-1,4 butadiene) system.[12] Table II summarizes the data on microheterophase structures for EBE block copolymers calculated from Eqs. (2), (3), and (4), together with the dimension D_{EM} estimated from electron micrographs.

Electron Microscopic Observation on Microheterophase Structures

Figure 5 illustrates the electron micrographs of EBE-10, EBE-20, EBE-40, and EBE-70 membranes cast from a mixture of CF-TFE (4 : 1 v/v). The domains of polybutadiene, stained with osmium tetroxide, correspond to the dark portions. Various microhetero-

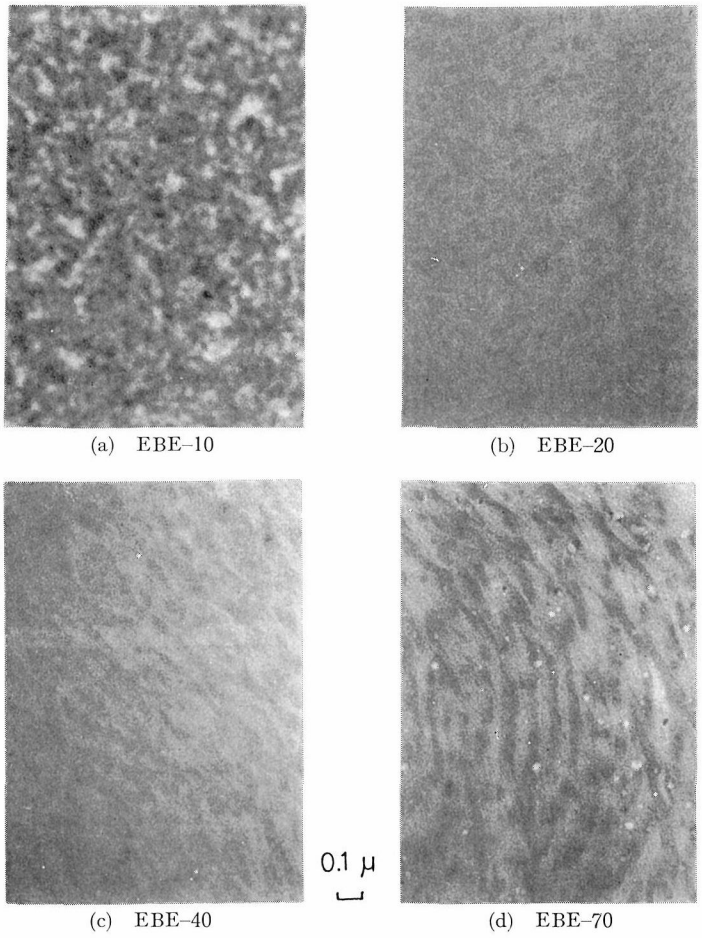

(a) EBE–10 (b) EBE–20

(c) EBE–40 (d) EBE–70

Fig. 5. Electron micrographs of EBE membranes cast from 4 : 1 CF-TFE at 25°C. Dark portions correspond to B domains. (×31,500)

phase structures are observed depending on the content of polybutadiene: a) EBE-10 takes an intermediate structure between sphere and cylinder, b) EBE-20 takes cylindrical structure, c) EBE-40 takes lamella-like structure, and d) EBE-70 takes inversed lamella-like structure, in which domains of PELG block exist in the matrix of polybutadiene.

Microheterophase structures were reported to be changed depending on compatibility of casting solvent composition in the mixtures of CF and TFE on microheterophase structure was examined on EBE-10 (see Fig. 6). As seen on the electron micrographs, light portions corresponding to PELG block increase with decreasing ratio of CF to TFE in the mixtures. As TFE is good solvent for PELG block in comparison with CF,[14] the molecular extension of PELG block in membrane appears to be enlarged with increasing ratio of TFE to CF in casting solvent.

Membrane Permeability

The permeation behavior of water through block copolymer membrane may be related closely to the microheterophase structure of the membrane. Permeability coefficient K of

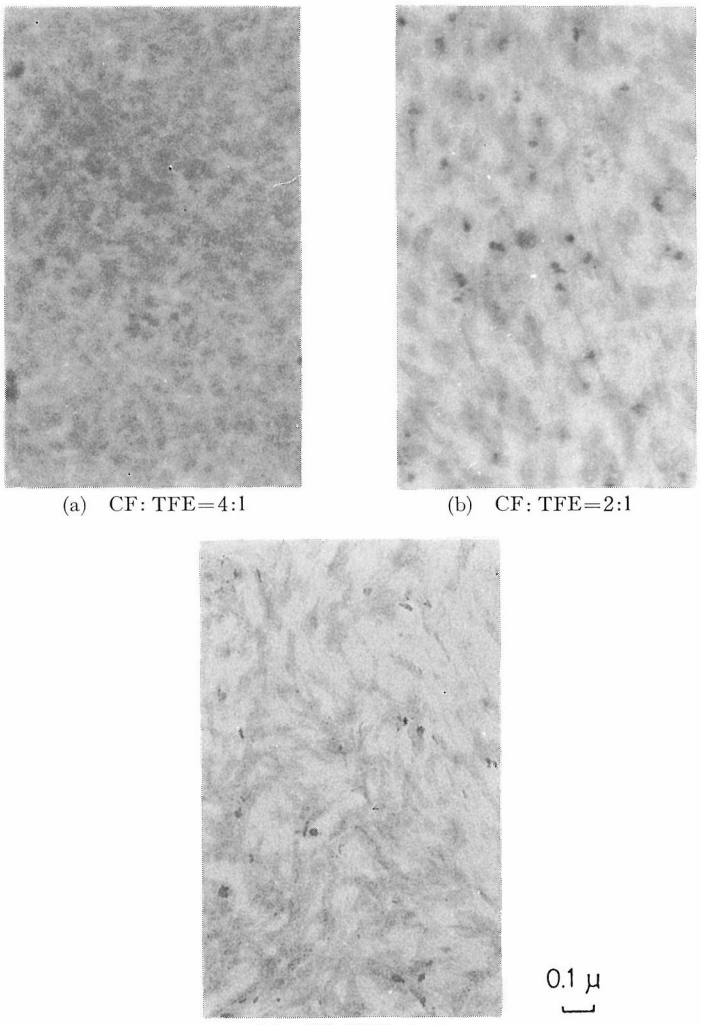

(a) CF: TFE=4:1 (b) CF: TFE=2:1

(c) CF: TFE=1:4

Fig. 6. Electron micrographs of EBE-10 cast from CF-TFE of different mixing ratios at 25°C. (×39,000)

a membrane of thickness ΔX under a hydraulic pressure difference Δp across the membrane is expressed by the following equation.[15]

$$K=\frac{V\eta}{At}\left(\frac{\Delta X}{\Delta p}\right) \tag{7}$$

where V, η, A, and t designate the volume of water, the viscosity of water, the area of membrane, and the time, respectively. If the water flux, J_f, per unit area of membrane is measured in unit time, Eq. (7) is written simply by Eq. (7').[16-19]

$$K=J_f\left(\frac{\Delta X}{\Delta p}\right) \tag{7'}$$

The relation between the water flux and the pressure difference at various temperatures

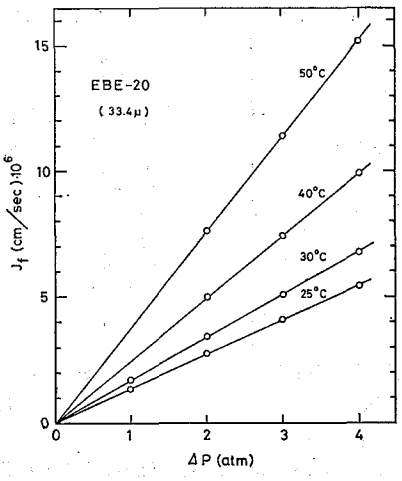

Fig. 7. Water flux J_f plotted against pressure Δp at various temperatures for EBE–20 membrane cast from 2 : 1 v/v CF-TFE mixture.

is illustrated in Fig. 7. In the pressure difference range examined, J_f is proportional to Δp, *i.e.*, the K values should be constant if the membrane compression is negligible under measured pressure just as the case of GBG block copolymer membranes. The permeability coefficient was calculated from the slope of those straight lines at given temperatures. The permeability coefficients of EBE block copolymer membranes at various temperatures are listed in Table III, in which those of MBM block copolymer membranes are also listed for comparison. Every membrane in Table III was cast from a mixture of CF and TFE (2 : 1 v/v).

Figure 8 shows the Arrhenius plot: $\log K$ plotted against $1/T$. The activation energies, calculated from the slopes, were 7.9 and 8.0 kcal/mole, respectively, for PELG and EBE-40. The activation energy of membrane permeation of MBM-11 was 8.2 kcal/mole and a little larger than that of PMLG, 7.6 kcal/mole. The activation energy of water

Table III. Water permeability coefficient K for PELG, EBE, PMLG, and MBM membranes at various temperatures

Sample code	ϕ_B	Thickness (μm) of membrane	$K\cdot10^9$ (cm^2/sec·atm) 25°C	30°C	40°C	50°C
PELG–2	0	20.1	3.10	3.83	5.72	8.64
EBE–05	0.17	23.3	3.56	4.28	6.13	9.43
EBE–10	0.28	27.0	3.75			
EBE–20	0.44	33.4	4.65	5.78	8.58	13.10
EBE–40	0.68	25.4	5.77	7.23	11.20	16.00
EBE–70	0.88	31.7	7.26			
PMLG–12	0	24.0	3.36	4.04	6.22	9.34
MBM–14	0.28	24.9	3.53	4.24	6.57	9.56
MBM–13	0.49	25.5	3.87			
MBM–12	0.65	25.0	4.43			
MBM–11	0.71	32.4	4.58	5.39	8.26	12.50

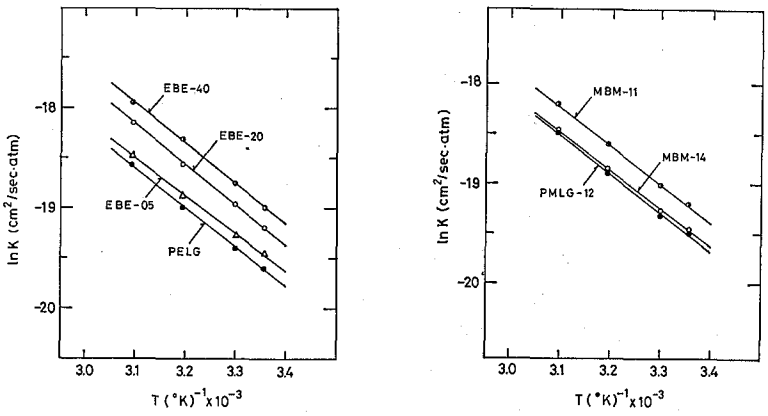

(a) (b)

Fig. 8(a). $\ln K$ plotted against 1/T for PELG and EBE series.
Fig. 8(b). $\ln K$ plotted against 1/T for PMLG and MBM series.

permeation of GBG block copolymer membranes was, accordingly, 2 to 3 times as large as those of EBE and MBM block copolymer membranes. The mechanism of water permeation of GBG seems to be different from that of EBE and MBM.

According to Chang *et al.*,[20] the permeability coefficient K is given from Fick's first law for steady state diffusion by Eq. (8).

$$K=\frac{D_w V_w \bar{v}}{RT} D_w V_w \tag{8}$$

where D_w is the diffusion coefficient of water inside the membrane, V_w is the volume fraction of water in the membrane, and $\bar{v}$ is the partial molar volume of water. The relation between the degree of swelling Q_w and the volume fraction of polybutadiene in membrane is summarized in Table IV, in which Q_w of membranes was measured after dipping mem-

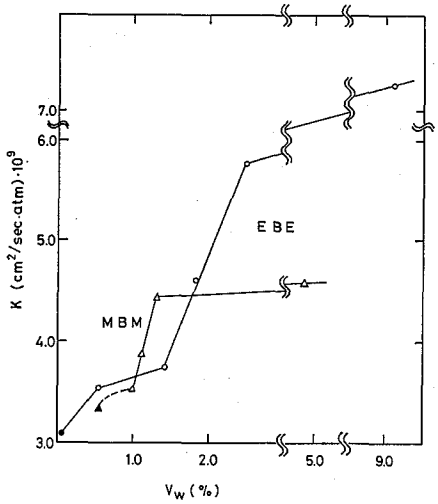

Fig. 9. Relation between K and V_w for EBE and MBM block copolymer membranes.

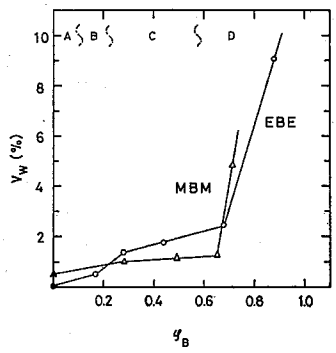

Fig. 10. Volume fraction, V_w, of water in membrane plotted against volume fraction, ϕ_B, of polybutadiene in nonswollen membrane.

branes in water for 48 h at 25°C.

Figure 9 shows the relation between K and V_w for EBE and MBM block copolymer membranes. The K values change stepwise with increasing V_w, which means that these block copolymer membranes should be regarded as heterogeneous membranes in permeation behavior. Such a change of K values corresponds to the microheterogeneity of block copolymer membranes. In Fig. 10, the volume fraction of water V_w in membrane is plotted against the volume fraction ϕ_B of polybutadiene in non-swollen membrane. i) In B region of Fig. 10, EBE-05 membrane has spherical domain structure. ii) In C region, EBE-20 and MBM-13 membranes have cylindrical domain structure. iii) EBE-40 and MBM-12 membranes have the domain structures inbetween cylindrical and lamella forms. iv) In D region, both EBE-70 and MBM-11 membranes have lamella structure in which polypeptide α-helix domains distribute in polybutadiene matrix, because of high content of polybutadiene. v) In A region, no microphase separation does occur.

It is curious phenomena that the high water fraction in membrane in the D region gave

Table IV. Degree of swelling Q_w of PELG, EBE, PMLG, and MBM membranes in water

Sample code	ϕ_B	Casting solvent CF : TFE	Thickness of membrane (μm) Dry	Wet	Q_w (%)
PELG–2	0	2 : 1	22.00	22.00	0.05
EBE–05	0.17	2 : 1	24.88	25.00	0.42
EBE–10	0.28	2 : 1	26.43	26.86	1.11
EBE–20	0.44	2 : 1	33.07	33.55	1.39
EBE–40	0.68	2 : 1	25.17	25.57	1.93
EBE–70	0.88	2 : 1	47.00	47.51	4.75
EBE–10	0.28	4 : 1	31.01	31.57	2.82
EBE–10	0.28	1 : 4	25.20	25.50	0.95
PMLG–12	0	2 : 1	26.15	26.22	0.43
MBM–14	0.28	2 : 1	26.07	26.55	0.78
MBM–13	0.49	2 : 1	20.05	20.50	0.88
MBM–12	0.65	2 : 1	25.00	25.50	1.01
MBM–11	0.71	2 : 1	31.00	32.15	3.78

Table V. Effect of casting solvents on membrane preparation

Sample code	Butadiene mole %	Casting solvent v/v	Q_w (%)
EBE-10	10.5	CF: TFE, 4 : 1	2.82
		CF: TFE, 2 : 1	1.11
		CF: TFE, 1 : 4	0.95
MBM-13	19.7	CF: TFA, 8 : 1	3.96
		CF: TFE, 2 : 1	0.88
MBM-12	31.9	CF: TFA, 8 : 1	4.71
		CF: TFE, 2 : 1	1.01

no high permeability. In homogeneous membrane, the permeability should increase linearly with increasing water fraction in membrane[19] and then exponentially in sufficiently high swollen membrane.[21] In anisotropic membranes made of styrene and 4-vinyl pyridine copolymers,[22] the exponential relation mentioned above was observed between the permeability and the water content in membranes. In EBE and MBM membranes of large ϕ_B, the water content of which is several %, there are some regions which play little role as channel for water permeation. The existence of water trap formed by structural distortion of hydrophobic polybutadiene matrix may be nominated for the immobile container of water, because PELG and PMLG are hydrophilic materials.

The effect of casting solvent on the degree of swelling in water is examined, as shown in Table V. A mixture of CF and TFE or TFA (trifluoroacetic acid) was used as casting solvent for membrane preparation. The larger CF content in casting solvent caused a higher degree of water swelling. In comparison with CF, TFE, which is a good solvent for PELG,[14] makes polypeptide component dispersed monomolecularly and results in a more closed packing in membrane, but it reduces the size of polybutadiene domains, as observed in electron micrographs in Fig. 6. In the membrane preparation of MBM, a minor amount of TFA in CF gives higher water swollen membranes. Since TFA changes α-helical conformation of polypeptides into partly random-coil conformation,[23] MBM membranes cast from a mixture of CF and TFA should have some random coil conformation, which seems to result in hgih degree of swelling of MBM block copolymer membrane. Thus the degree of water swelling of EBE and MBM block copolymer membranes cast from TFA, CF, and TFE are in the following order: TFA$\gg$CF$>$TFE.

Let's discuss the mechanism of water permeation in microheterophase structure membranes of block copolymers composed of polypeptides and polybutadiene. Such microheterophase membranes are assumed to be composed of several regions: i) relatively hydrophilic polypeptide domain region composed of α-helical chains, ii) hydrophobic polybutadiene domain region, iii) hydrophilic interfacial region[3] existing inbetween polypeptide domain and polybutadiene domain, and iv) the space surrounded by micelles of sphere, cylinder, or lamella form, *i.e.*, a kind of microvoid. These regions should have different water permeabilities. It was pointed out[20] that these different mechanisms of water permeation give additive contribution to the permeability coefficient of membrane. Eventually, the permeability coefficient K of microheterophase structure membrane is given by Eq. (9).

$$K=K_A\phi_A+K_{intf}\phi_{intf}+K_B\phi_B+K_v\phi_v \tag{9}$$

where the subscript A, intf, B, and v denote polypeptide, interfacial, polybutadiene, and microvoid regions, respectively.

With respect to A–B–A block copolymer membranes, the polybutadiene domain is considered to take no part in water permeation because of its hydrophobicity. This means that K_B can be negligible. As summarized in Table III, permeability coefficients are in the order of 10^{-9} cm^2/sec·atm for EBE and MBM block copolymer membranes, from which it is anticipated that water permeates by means of diffusion flow in these membranes, so-called dense membrane. For example, the radius[24] r of pore in swollen membrane can be estimated by Eq. (10) from Poiseuille's law and the method of Manegold,[25] assuming that water channel of membrane is of cylindrical form to the direction of permeation.

$$r=\sqrt{3\cdot 8\eta\, l^2K/Wg} \tag{15}$$

where K is the permeability constant in c.g.s. unit, l is the thickness of swollen membrane, W is the water fraction in membrane per unit membrane area, and g is the accerelation of the gravity. The radius of pore in EBE-05 membrane was calculated to be 2.74 Å, which supports the prediction that the water permeation of the membrane is driven by the diffusion flow, and that there exists no microvoid surrounded by micelles in EBE and MBM block copolymer membranes. Thus the term $K_v\phi_v$ is omitted, and Eq. (9) is written as Eq. (9') for EBE and MBM block copolymer membranes.

$$K=K_A\phi_A+K_{intf}\phi_{intf} \tag{9'}$$

As ϕ_{intf} is so small compared with ϕ_A and ϕ_B, it may be assumed in the first approximation that $\phi_A+\phi_B=1$.

In Figure 11, the values of $K_{intf}\phi_{intf}$ are plotted against $\phi_B^{4/3}$. Good linear relation between $K_{intf}\phi_{intf}$ and $\phi_B^{4/3}$ is seen for EBE and MBM block copolymer membranes. If ϕ_{intf} is regarded to be proportional to $\phi_B^{2/3}$, the K_{intf} increases with $\phi_B^{2/3}$, which is

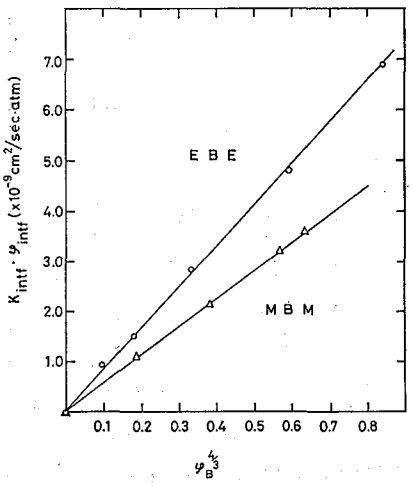

Fig. 11. $K_{intf}\phi_{intf}$ plotted against $\phi_B^{4/3}$ for EBE and MBM block copolymer membranes.

in accordance with the dimension of area of the interfacial region. In other words, the thickness of interfacial region is considered to be constant, regardless of structural change of micelles.

From the results mentioned above, the following conclusion was derived on the water permeability of polypeptide membranes: i) Water permeation in both PMLG and PELG membranes takes place in side chain region among polypeptide α-helices, and K_A of PMLG is larger than that of PELG, as shown in Fig. 9 and Table IV. Such conclusion is in accord with the results of Takizawa *et al.*[26,27] and Minoura and Nakagawa[23] that water vapor diffuses and permeates through the side chain regions among α-helices of PMLG membrane. ii) From the slopes of two straight lines in Fig. 11. K_{intf} of EBE is thought to be larger that those of MBM, which is attributed to the longer side chain of PELG than of PMLG and to the better compatibility of ethyl group with polybutadiene than that of methyl group having better crystallinity in block copolymer membranes. iii) Taking into consideration that K value of GBG membranes was in the order of 10^{-6} cm²/sec·atm, the GBG membranes should have space, *i.e.*, microvoids among micelles. Benzyl group has worse compatibility with polybutadiene, and the crystallinity of the GBG membranes is better than that of EBE. Accordingly, the micelles formed in GBG membranes is of more well-defined form than those of EBE membranes. The aggregation of GBG molecules causes no structural disorder of micelles and results in the formation of well-defined micelles, while better orientation of rigid rod-like α-helices and of bulky benzyl groups may result in microvoid: iv) Finally, the permeability coefficients, K_A, K_{intf}, K_B, and K_v for polypeptide block copolymer membranes are in the following order:

$$K_v \gg K_{intf} > K_A > K_B \simeq 0$$

Takizawa *et al.*[28] reported that a series of alcohols permeate through the side chain region among helices of PMLG, and the diffusion coefficient decreased systematically with increasing molecular size of penetrants. Similar tendency is obtained for the permeation

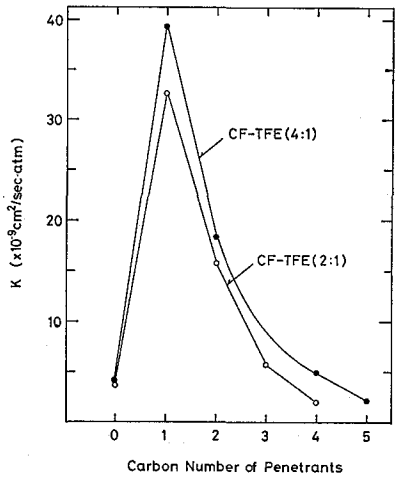

Fig. 12. Permeability coefficient plotted against carbon number of alcohol penetrants: 0, H_2O; 1, methyl alcohol; 2, ethyl alcohol; 3, *n*-propyl alcohol; 4, *n*-butyl alcohol; 5, *n*-amyl alcohol.

Table VI. K of EBE membrane cast from mixture of CF : TFE (4 : 1 v/v)

Permeant	PELG	EBE-05	EBE-10	EBE-20
CH_3OH	26.4		39.4	
C_2H_5OH	8.04	12.9	18.4	23.9

of alcohol penetrants in EBE-10 membrane, as illustrated in Fig. 12. Table VI shows the permeability coefficient of EBE membranes for alcohols, which increases with polybutadiene content. Alcohol molecules appear to permeate not only through side chain region of α-helices but also through the interfacial region between polybutadiene and polypeptide.

Biocompatibility

The tissue compatibility of EBE block copolymer materials was examined, and the results are listed in Table VII, where the level to evaluate the biocompatibility of materials is as follows[6]:

(−); cells do not recognize as foreign body.
(±); inbetween recognition of (−) and (+) by cells.
(+); cells recognize as foreign body, giant cells and fibroblasts gather close to the test materials, and cell layers less than 10 surround the foreign body, which corresponds light foreign body reaction.
(++); inbetween reaction of (+) and (+++).
(+++); multiple layers of cells like a lump gather close to the test material, which is remarkable foreign body reaction.
(++++); the test material works as poison to cells, which causes necrosis.

The degree of absorbance by living body is evaluated according to the following bases[6]:

(−); no absorbance or scarcely low absorbance is observed.
(+); about 25% of test material is absorbed.
(++); about 50% of test material is absorbed.
(+++); about 75% of test material is absorbed.
(++++); more than *ca.* 95% of test materials is absorbed.

In comparison with MBM, GBG, and LBL (block copolymers containing poly(ε-N-carbobenzyloxy L-lysine), it is surprising that the foreign body reaction and the degree of absorbance of EBE was low. As seen on microscope photographs of polymer samples and surrounding tissue in Fig. 13, not so remarkable foreign body reaction can be observed in the case of PELG, EBE, and PB as inflamatory cell infiltration and granulomatous

Table VII. Biocompatibility of EBE materials

Sample	Foreign body reaction	Absorbance by living body
PELG	+	−
EBE-05	±	− or +
EBE-10	+	− or +
EBE-20	±	−
EBE-40	+	−

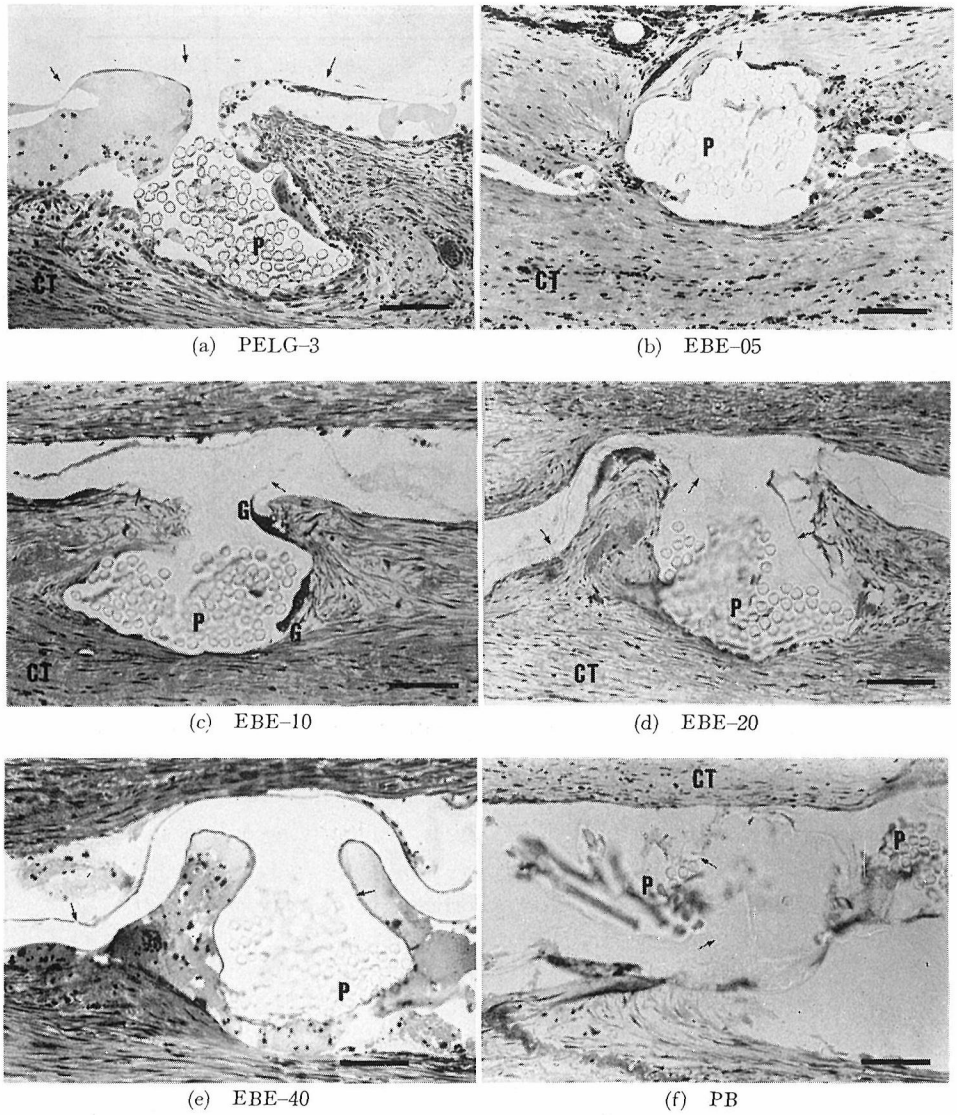

(a) PELG-3 (b) EBE-05

(c) EBE-10 (d) EBE-20

(e) EBE-40 (f) PB

Fig. 13. Microscope photographs of samples and surrounding tissue: P, polyester fiber; G, giant cell; CT, connective tissue; arrow, sample material. Bar indicates 100 μm.

tissue was observed in the case of both LBL and MBM having cylindrical structure, and GBG having lamellalike structure. Ethyl ester is considered not only to have special biocompatibility, but also to contribute to the worse ordering structure of EBE because of bad crystallinity. Thus, EBE looks a promising material for biomedical applications.

ACKNOWLEDGMENT

The authors wish to thank Daikin Kogyo Co. for taking electron micrographs, Prof.

Matsumoto in Kobe University for a wide-angle X-ray diffraction measurement, and Prof. Kitamaru for a microbalance measurement.

REFERENCES

(1) A. Nakajima, T. Hayashi, K. Kugo, and K. Shinoda, *Macromolecules*, **12**, 840 (1979).
(2) A. Nakajima, K. Kugo, and T. Hayashi, *Macromolecules*, **12**, 844 (1979).
(3) A. Nakajima, K. Kugo, and T. Hayashi, *Polymer J.*, **11**, 995 (1979).
(4) G-W. Chen, T. Hayashi, and A. Nakajima, *Polymer J.*, **14**, 433 (1981).
(5) T. Hayashi, K. Kugo, and A. Nakajima, *Contemporary Topics in Polymer Science*, **4**, Plenum Press, N.Y., in press, 1981.
(6) Y. Noishiki, Y. Nakahara, H. Sato, and A. Nakajima, *Artif. Organs*, **9**, 678 (1980).
(7) Y. Uematsu, *Polymer J.*, **6**, 431 (1974).
(8) C. H. Bamford and W. E. Hanby, *Nature*, **169**, 120 (1952).
(9) G. Valle, A. Del Pra, P. Spadon, and M. Mami, *Biopolymers*, **14**, 437 (1975).
(10) F. T. Wall, *J. Chem. Phys.*, **11**, 67 (1943).
(11) M. Kurata, Y. Uchiyama, T. Koyama, and H. Fujita, Rept. 12th Polym. Symp. of Soc. Polym. Sci., Japan, Nov. 5 (1963).
(12) A. Nakajima, K. Kugo, T. Hayashi, and H. Sato, *Kasen Koenshu*, **36**, 125 (1979).
(13) A. Nakajima and T. Korenaga, *Bull. Inst. Chem. Res., Kyoto Univ.*, **52**, 295 (1974).
(14) M. Terbojevich, E. Peggion, A. Cosani, G. D'Este, and E. Scoffone, *European Polym. J.*, **3**, 681 (1967).
(15) M. F. Refojo, *J. Appl. Polym. Sci.*, **11**, 1991 (1967).
(16) H. Yasuda, C. E. Lamaze, and A. Peterlin, *J. Polym. Sci., A-2*, **9**, 1117 (1971).
(17) H. Yasuda and C. E. Lamaze, *J. Polym. Sci., A-2*, **9**, 1537 (1971).
(18) H. Yasuda, C. E. Lamaze, and A. Schindler, *J. Polym. Sci., A-2*, **9**, 1579 (1971).
(19) A. Perterlin, H. Yasuda, and H. G. Olf., *J. Appl. Polym. Sci.*, **16**, 865 (1972).
(20) Y. J. Chang, C. T. Chen, and A. V. Tobolsky, *J. Polym. Sci., Polymer Phys. Ed.*, **12**, 1 (1974).
(21) H. Yasuda and L. D. Ikenberry, *J. Appl. Polym. Sci.*, **15**, 2841 (1971).
(22) J. L. Williams, A. Schindler, and A. Perterlin, *Makromol. Chem.*, **147**, 175 (1971).
(23) M. Minoura and T. Nakagawa, *J. Appl. Polym. Sci.*, **23**, 2729 (1979).
(24) I. Sakurada, A. Nakajima, and H. Takita, *Kobunshi Kagaku*, **10**, 522 (1954).
(25) E. Manegold *et al.*, *Koll.-Z.*, **43**, 5 (1927), **49**, 372 (1929), **50**, 22 (1930), **50**, 207 (1930).
(26) A. Takizawa, T. Hamada, and J. Shimozawa, *Kobunshi Kagaku*, **28**, 751 (1971).
(27) A. Takizawa, T. Hamada, H. Okada, S. Kadota, and H. Nonoyama, *J. Appl. Polym. Sci.*, **18**, 1443 (1974).
(28) A. Takizawa, T. Hamada, H. Okada, S. Imai, and S. Kadota, *Polymer*, **15**, 157 (1974).